ISSN 1068-3666, Journal of Friction and Wear, 2010, Vol. 31, No. 4, pp. 308–316. © Allerton Press, Inc., 2010.
Original Russian Text © A.V. Khomenko, I.A. Lyashenko, 2010, published in Trenie i Iznos, 2010, Vol. 31, No. 4, pp. 412–422.

A Stochastic Model of Stick-Slip Boundary Friction with Account for the Deformation Effect of the Shear Modulus of the Lubricant

A. V. Khomenko and I. A. Lyashenko*

Sumy State University, ul. Rimskogo-Korsakova 2, Sumy, 40007 Ukraine

**e-mail: nabla04@ukr.net*

Received July 8, 2009

Abstract—The melting of an ultrathin lubricating film during the friction of two solid atomically smooth surfaces is studied within the limits of the Lorentz model that approximates a viscoelastic medium, the deformation effect of the shear modulus being taken into account. It is shown that the action of a random force representing additive non-correlated noise results in the sustained oscillation mode that corresponds to stick-slip friction. The numerical modeling of the process yields the ratios between the relaxation times at which the stick-slip mode is characterized by a high amplitude. The amplitude of stick-slip transitions is found to decrease as the shear modulus of the lubricant increases.

Key words: lubricant, stick-slip friction, white noise, shear modulus, adiabatic approximation, Lorentz system, oscillations, shear stresses.

DOI: 10.3103/S1068366610040100

INTRODUCTION

During recent decades researchers have taken a keen interest in studies of the friction of molecularly thin lubricating layers pressed between two atomically smooth solid surfaces [1–3] under various applied loads and pressures and for various layer thicknesses, shear rates, temperatures, etc. The aim of the present study is to investigate the tribological and rheological properties of ultrathin lubricating layers, which differ qualitatively from the layers' bulk properties. The necessity of studying these differences results from the development of nanotechnologies, with the consequent growing demand for small-sized tribosystems. Such friction units have found application in modern storage devices, aerospace facilities, miniature motors, microelectronic positioning systems, etc. We note that similar behavior of the lubricants is observed in almost all real mechanisms; it is caused by the squeezing-out of the lubricant from the contacting surfaces under the effect of the applied load. Boundary friction has been studied experimentally [1–3] and theoretically [4–7], as well as by computer simulation [8]. It has been found that, as the lubricating layer thickness decreases during friction, the physical properties of the layers first change quantitatively and then the variations acquire a pronounced qualitative pattern. In particular, it has been shown that under steady friction the behavior of a lubricating layer may correspond to a multiphase state that induces stick-slip friction, i.e., transitions between solidlike and fluidlike states of the lubricant. However, especially for chain molecules like hexadecane, the fluidlike state differs strongly from the basic state of the fluid. Of primary interest are the dynamic properties of the layers in the boundary mode, when transitions between different types of dynamic states occur during sliding. Recent studies of the sliding of mica and quartz surfaces lubricated with various substances such as metal monolayers, organic fluids, and water, have shown that these phase transitions are the rule rather than the exception. They appear as stick-slip motion that is characterized by transitions between two or more dynamic states. Insight into the mechanisms of stick-slip friction is important for tribologists since it is one of the main causes of the wear and damage of rubbing parts. However, stick-slip friction is a more general phenomenon. For example, it causes the sounds of a violin, the creaking of a door, the boom of machinery, etc. Studies of the properties of ultrathin layers necessitate special high-technology equipment due to their nanometer thicknesses. Nevertheless, despite the intricacy of the problem, there are experimental devices and corresponding techniques [9] for measuring the thickness and viscosity of molecular layers, the friction coefficient, the shear components of viscous and elastic stresses, etc.

The authors of paper [7] proceeded from the rheological description of a viscoelastic medium possessing thermal conductivity and derived a system of kinetic equations that governed the mutually coordinated behavior of the shear components of the stresses σ and the relative deformation ε arising in an ultrathin lubricating film, as well as the lubricant temperature T, during the friction of two atomically smooth solid surfaces. Within the limits of that theory, the effect of additive non-correlated noises on lubricant melting

has been studied [10], melting due to dissipative effects has been considered [11], temperature correlations [12] and various temperature dependences of the viscosity [13] have been taken into account, and hysteresis phenomena at melting have been investigated [14, 15]. However, these papers report a stochastic stick-slip mode when the static and kinetic friction forces vary chaotically with time. Though the stick-slip mode of boundary friction has been established both experimentally [16] and by using methods of molecular dynamics [8], more often it is of a periodical pattern [1, 5, 6, 8]. The present study is aimed at elucidating the causes and specific features of this mode within the limits of the rheological model [7] with account for the deformation effect of the shear modulus that always exists. The paper is theoretical and rather qualitative since the friction surfaces are assumed to be perfectly smooth and infinite and the lubricant is assumed to be homogeneous. Nevertheless, staying within the limits of this approach, we succeeded in finding the causes of the stick-slip motion of the sheared surfaces and considering the main specific features of boundary friction that are observed experimentally. These features are the action of elastic stresses in the fluid-like phase, lubricant melting due to the shear of the friction surfaces with increasing stresses, melting that starts when the temperature exceeds its critical value T_{c0}, the occurrence of stick-slip friction, etc. We note that the application of the model under consideration is restricted by the critical lubricating layer thickness [7], which depends on the parameters of the lubricant; if the lubricating layer thickness exceeds its critical value, the equations discussed below become inapplicable.

STICK-SLIP MODE

Let us write down the system of equations for the shear components of the stresses σ and the strain ε, as well as for the temperature T, using the units [7, 10–15, 17]

$$\sigma_s = \left(\frac{\rho c_v \eta_0 T_c}{\tau_T}\right)^{1/2}; \quad \varepsilon_s = \frac{\sigma_s}{G_0}; \quad T_c \qquad (1)$$

for the variables σ, ε, and T, respectively, where ρ is the lubricant density; c_v is the lubricant specific heat; T_c is the critical temperature; $\eta_0 \equiv \eta$ at $T = 2T_c$ is the characteristic value of the shear viscosity η; $\tau_T \equiv \rho l^2 c_v/\kappa$ is the thermal conductivity time; l is the lubricating layer thickness; κ is the thermal conductivity of the lubricant; τ_ε is the relaxation time of strain; and $G_0 \equiv \eta_0/\tau_\varepsilon$ is the characteristic value of the shear modulus:

$$\tau_\sigma \dot{\sigma} = -\sigma + g(\sigma)\varepsilon; \qquad (2)$$

$$\tau_\varepsilon \dot{\varepsilon} = -\varepsilon + (T-1)\sigma; \qquad (3)$$

$$\tau_T \dot{T} = (T_e - T) - \sigma\varepsilon + \sigma^2. \qquad (4)$$

Here we have introduced the relaxation times of the stresses τ_σ and the temperature τ_T, as well as the temperature of the friction surfaces T_e and the function $g(\sigma) \equiv G(\sigma)/G_0$, where $G(\sigma)$ is the shear modulus of the lubricant, which depends on the stresses as follows:

$$G(\sigma) = \Theta + \frac{G - \Theta}{1 + (\sigma/\sigma_p)^\beta}, \quad \beta = \text{const} > 0. \qquad (5)$$

At $g(\sigma) = G/G_0 \equiv \text{const}$, equation (2) reduces to a relation like the Maxwell equation for describing a viscoelastic medium by substituting ε/τ_σ for $\partial\varepsilon/\partial t$. The Maxwell equation implies the use of the idealized Henky model. For the dependence of the stresses on the strain $\sigma(\varepsilon)$, this model is presented by the Hooke law $\sigma = G\varepsilon$ at $\varepsilon < \varepsilon_m$ and by the constant $\sigma_m = G\varepsilon_m$ at $\varepsilon \geq \varepsilon_m$. Here, σ_m and ε_m are the maximal values of the shear stresses and the shear strain for the Hooke portion; $\varepsilon > \varepsilon_m$ results in viscous flow with the deformation rate $\dot{\varepsilon} = (\sigma - \sigma_m)/\eta$. In fact, the curve $\sigma(\varepsilon)$ contains two portions. The first, Hooke portion has a high slope angle that is governed by the shear modulus G. The next portion is the much flatter portion of plastic deformation, whose slope angle depends on the strengthening factor $\Theta < G$. This situation apparently means that the shear modulus depends on the stresses. To take this into account we have used the simplest approximation (5) that describes the above-mentioned transition from elastic deformation to plastic.

The substitution of relation (5) into (2) transforms the dependence $g(\sigma)$ into the following equality [15, 17]:

$$g(\sigma) = g_\theta\left(1 + \frac{\theta^{-1} - 1}{1 + (\sigma/\alpha)^\beta}\right), \qquad (6)$$

where we have introduced the parameter $\theta = \Theta/G < 1$ that governs the ratio of the slope angles of the deformation curve within the plastic and Hooke portions and the coefficients $g_\theta = \Theta/G_0 < 1$ and $\alpha = \sigma_p/\sigma_s$.

In our previous papers [7, 10–15, 17], we have shown that the zero stationary stresses σ_0 correspond to the solidlike structure of the lubricant, while at $\sigma_0 \neq 0$ the latter melts and transits to a liquidlike state, which corresponds to the plastic flow portion of the loading diagram. Transitions between the liquidlike and solidlike structures are represented as phase transitions, but between different kinetic friction modes rather than between equilibrium thermodynamic phases; several kinetic friction modes may exist [1]. At this approach the shear modulus of the lubricant is an effective value that, similar to the common shear modulus, is expressed through the tangent of the slope angle of the loading curve $\sigma(\varepsilon)$ within its Hooke portion. In paper [4] the shear modulus of thin lubricating films is represented as the squared amplitude of the periodical portion of the microscopic function of the medium density; in the fluid state, the function is homogeneous and the shear modulus is equal to zero, while in the solid state it is periodical and the shear modulus is

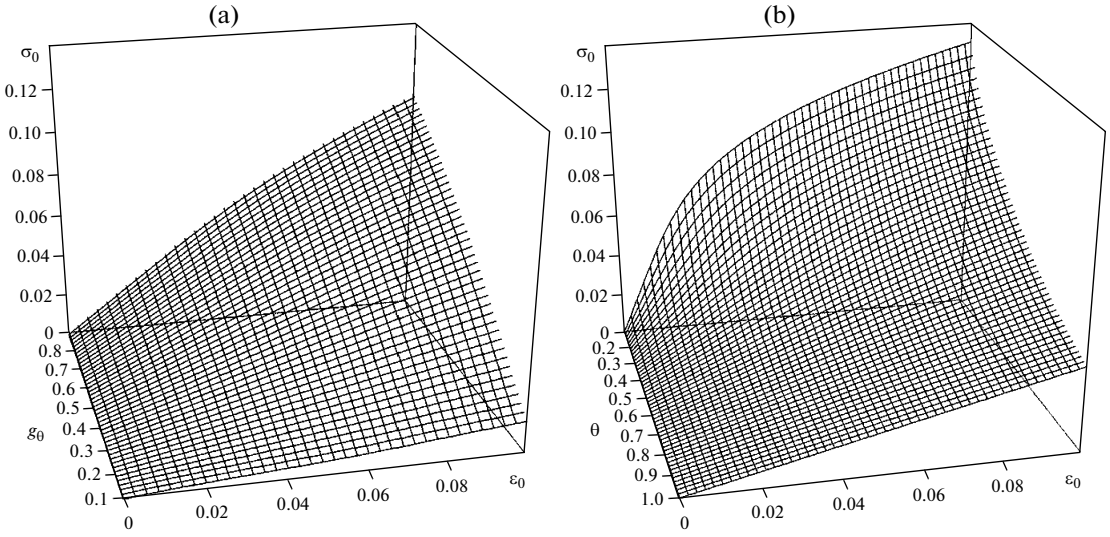

Fig. 1. Dependence of stationary value of shear stresses σ_0 on strain ε_0 (equation (7)) at $\alpha = 0.1$ and $\beta = 4$, on coefficient g_θ at $\theta = 0.7$ (a), and on coefficient θ at $g_\theta = 0.4$ (b).

nonzero. However, here we consider solidlike and fluidlike states rather than solid and fluid phases; this is why the fluidlike state can also be characterized by a nonzero shear modulus and the presence of the elastic component of stresses.

In the stationary case $\dot\sigma = 0$, equation (2) yields the generalized Hooke law

$$\sigma_0 = g(\sigma_0)\varepsilon_0, \qquad (7)$$

where the shear modulus depends on the stresses. The dependence $\sigma_0(\varepsilon_0)$ is called the loading curve and is shown in Fig. 1 in three-dimensional coordinates. As is seen in Fig. 1a, with increasing parameter g_θ, the angle of slope of the Hooke and plastic portions of the curve $\sigma_0(\varepsilon_0)$ relative to the ε_0 axis increases, corresponding the a lubricant with a higher shear modulus. Figure 1b shows that with decreasing parameter θ, the difference between the Hooke portion and the plastic flow portion becomes more pronounced. Particular values of the parameters g_θ and θ are selected for further analysis.

In time, all the derivatives in equations (2)–(4) become zero and the lubricant characteristics do not change; this corresponds to the stationary state. Depending on the surface temperature T_e, either dry ($\sigma_0 = 0$) or fluid ($\sigma_0 \neq 0$) friction may occur. Equating of the derivatives to zero yields the following equation:

$$\frac{(1+(\sigma/\alpha)^\beta)(1+\sigma^2)}{\theta^{-1}+(\sigma/\alpha)^\beta} - g_\theta(T_e - 1 + \sigma^2) = 0. \qquad (8)$$

With arbitrary constants, it can not be solved analytically for σ and can be examined only numerically. However, it presents the analytical dependence $T_e(\sigma)$ and can be used to plot the dependence of the stationary stresses on the temperature $\sigma_0(T_e)$ from the dependence $T_e(\sigma_0)$. Such analysis shows that, depending on the parameters, the phase transition of either the second or the first order may occur in the system [15, 17]. The behavior of the system until the stationary state is reached is strongly governed by the ratios between the relaxation times. Below, we consider the boundary cases, when one of the relaxation times can be assumed small.

The case $\tau_T \ll \tau_\sigma, \tau_\varepsilon$. Let us assume $\tau_T \dot T \approx 0$ in equation (4) [18], find T from it and substitute the result in (3); this yields two-parameter system (2), (3). Then we reduce the two derived first-order differential equations, which depend on the stress σ and the strain ε, to one second-order equation for σ. For this purpose, we should express ε through σ in (2) and write the derivative of the resulting expression with time. Then we substitute the derived dependences $\varepsilon(\sigma, \dot\sigma)$, and $\dot\varepsilon(\sigma, \dot\sigma)$ into (3) and find the required equation. If the time is measured in units of τ_σ, the equation has the following form:

$$\ddot\sigma + [A\dot\sigma + A\sigma + 1 + \tau^{-1}(1+\sigma^2)]\dot\sigma + B\sigma = \xi(t);$$
$$A \equiv \frac{\beta(\theta^{-1}-1)\sigma^{\beta-1}}{\alpha^\beta[\theta^{-1}+(\sigma/\alpha)^\beta][1+(\sigma/\alpha)^\beta]}; \qquad (9)$$
$$B \equiv \frac{1+\sigma^2}{\tau} - \frac{g_\theta[\theta^{-1}+(\sigma/\alpha)^\beta](T_e - 1 + \sigma^2)}{\tau[1+(\sigma/\alpha)^\beta]},$$

where $\tau = \tau_\varepsilon/\tau_\sigma$.

Equation (9) is determinate and does not take into account the spatial inhomogeneity such as surface roughness, presence of impurities in the lubricant, etc. As a rule, in real experimental systems, fluctuations occur, which are typically described by noises with

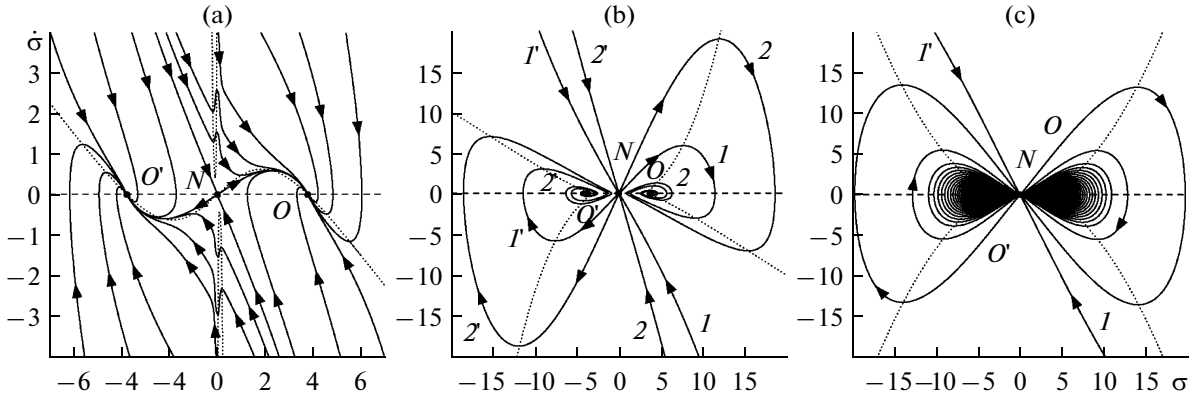

Fig. 2. Phase-plane portraits of system at values of parameters $\theta = 0.7$, $g_\theta = 0.4$, $\alpha = 0.1$, $\beta = 4$, and $T_e = 25$ and at noise intensity $D = 0$, which represent (a) solution of equation (9) at $\tau = \tau_\varepsilon/\tau_\sigma = 15$; (b) solution of equation (15) at $\tau = \tau_T/\tau_\sigma = 120$; and c—solution of equation (16) at $\tau = \tau_T/\tau_\varepsilon = 120$.

various correlation times and frequency ranges. The noises are considered when solving a problem with a great number of inhomogeneities, defects, external effects, etc., in the case when all of the existing effects cannot be described adequately. A striking example is Brownian motion—collisions of molecules described by Newtonian mechanics are seen at the microlevel. At the macrolevel, chaotic motion is observed due to the huge number of collisions per unit time; it cannot be described correctly. However, if one writes down the Langevin equation with noise, it is possible to predict analytically the probability of the presence of a particle within a specific coordinate domain. In this paper, we consider a thin lubricating layer consisting of a restricted number of molecules. In this case, fluctuations of the values that are insignificant for macroscopic bulk lubricants will affect strongly the friction characteristics. Fluctuations may also result from imperfections of the test devices used in a particular experiment, external effects, inhomogeneities, etc. To take these effects into account, we additionally consider the influence of the random force $\xi(t)$ in (9). It represents white noise and has the moments

$$\langle \xi(t) \rangle = 0; \quad \langle \xi(t)\xi(t') \rangle = 2D\delta(t - t'), \qquad (10)$$

where D plays the role of a stochastic source.

Let us represent (9) in the canonical form:

$$\ddot{\sigma} + 2\gamma\dot{\sigma} + \omega_0^2\sigma = \xi(t), \qquad (11)$$

where the attenuation factor γ and the fundamental frequency of oscillations ω_0 depend on the stresses. Since a constant value of the stresses ($\dot{\sigma} = 0$) is reached in the system in the stationary state at $D = 0$, it can be found by equaling the last term of the left-hand side of (9) to zero, yielding (8). This corresponds to oscillations with the zero frequency ω_0.

To solve equation (11) numerically, we make the substitution $y = \dot{\sigma}$, yielding

$$\begin{aligned} \dot{\sigma} &= y; \\ \dot{y} &= -2\gamma y - \omega_0^2\sigma + \xi(t), \end{aligned} \qquad (12)$$

where γ and ω_0 follow from the comparison of (9) and (11). Then we use the Euler method for integration. In this case, the iteration procedure is as follows [11, 12]:

$$\begin{aligned} \sigma_2 &= \sigma_1 + y_1\Delta t; \\ y_2 &= y_1 + (-2\gamma y_1 - \omega_0^2\sigma_1)\Delta t + \sqrt{\Delta t}W_n. \end{aligned} \qquad (13)$$

We use the Box–Muller model [19] to simulate the random force W_n:

$$W_n = \sqrt{2D}\sqrt{-2\ln r_1}\cos(2\pi r_2), \quad r_i \in (0, 1], \qquad (14)$$

where the pseudorandom numbers r_1 and r_2 are uniformly distributed.

The numerical solution of equation (9) obtained using procedure (13), (14) is presented in Fig. 2a in the form of a phase-plane portrait. Here, the isocline along which $\dot{\sigma} = 0$ is shown by the dashed line and the phase trajectories have the vertical tangent. This isocline is the abscissa axis of the coordinates under consideration. The dotted line represents the isocline $\ddot{\sigma} = 0$, along which the phase trajectories have the horizontal tangent. Since the attenuation factor in (9) depends on $\dot{\sigma}$ when $\ddot{\sigma} = 0$ equals zero, the expression for the isocline $\dot{\sigma}(\sigma)$ is found from the solution of the quadratic equation; this is why the dependence is binary. The figure shows that the following three singular points exist: the saddle N in the origin, which is unstable since it corresponds to the maximum of the synergetic potential [7], and two stable points O and O' that are symmetrical relative to the value $\sigma = 0$. A tendency to the oscillation process is observed in the vicinity of these points when the stationary value of σ_0

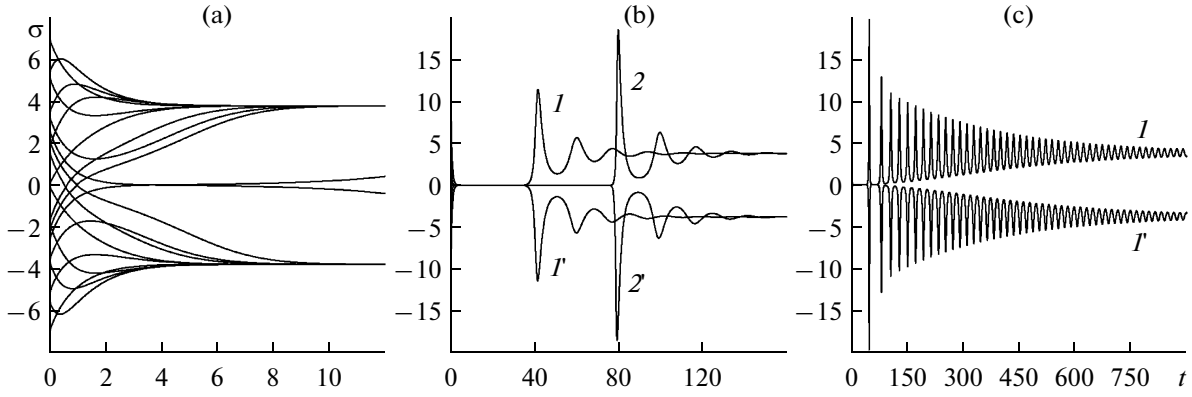

Fig. 3. Time dependences of stresses that correspond to phase-plane portraits shown in Fig. 2.

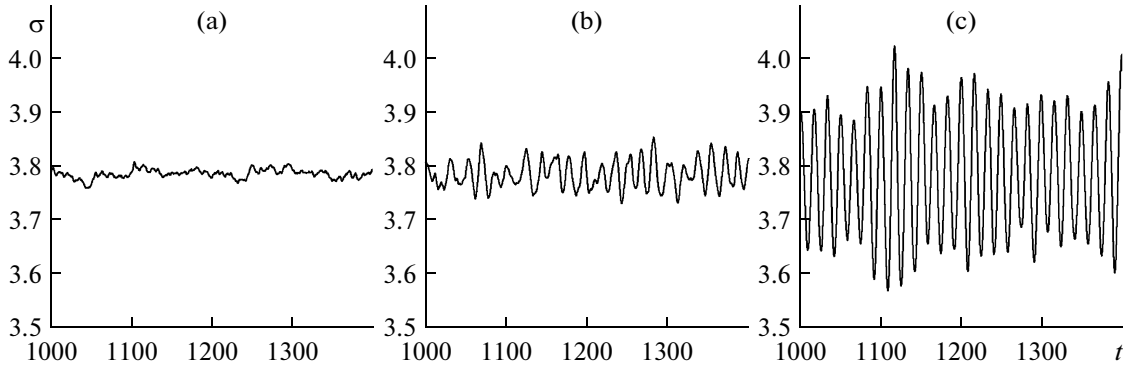

Fig. 4. Time dependences of stresses that correspond to phase-plane portraits shown in Fig. 2 and to time dependences of the stresses shown in Fig. 3 at noise intensity $D = 10^{-5}$.

is reached; however, the process does not occur since the attenuation factor is high. For the considered ratio between the relaxation times, such behavior appears within the whole range of the parameters [17]. We note that positive and negative values of the stresses correspond to the motion of the upper friction surface in different directions. Thus, at a positive initial value of σ, which is proportional to the shear rate, and a negative initial value of $\dot{\sigma}$ or acceleration, reciprocal motion may occur, as follows from the figure.

Figure 3a illustrates the time dependences of the stresses, which correspond to the trajectories shown in Fig. 2a. The dependences present the nonperiodic transient mode, when values of the stresses vary until a constant sliding velocity is reached ($\sigma = \text{const}$).

Figure 4a shows the solution of the same equation as Fig. 3a but at $D \neq 0$. It is seen that with time the stresses vary randomly, yet within a narrow range since the noise intensity is low; this corresponds to the sliding mode. The dependence is presented starting from the moment $t = 1000$ since in this study we consider the stationary friction mode rather than the transient one.

Figure 5a illustrates the dependence of the power of the signal presented in Fig. 4a on its frequency. It is seen that at low frequencies $S(\nu) = \text{const}$ and then the power decreases. The decrease results from the fact that equation (9) for white noise $\xi(t)$ is a filter that does not pass high frequencies and gives certain color to the noise. The dependence $S(\nu)$ contains no pronounced maxima, which proves the absence of the periodical component in the dependence $\sigma(t)$. Thus, in this case the sliding mode with a slightly fluctuating shear rate becomes more steady with time.

The case $\tau_\varepsilon \ll \tau_T$, τ_σ. In this case, we use the approximation $\tau_\varepsilon \dot{\varepsilon} \approx 0$ in the original system; if the time is measured in units of τ_σ, this yields the following equation:

$$\ddot{\sigma} + [(A - \sigma^{-1})\dot{\sigma} + A\sigma + \tau^{-1}(1 + \sigma^2)]\dot{\sigma} + B\sigma = \xi(t), \quad (15)$$

where the ratio $\tau = \tau_T/\tau_\sigma$ is introduced and the coefficients A and B are determined in (9).

The phase-plane portrait resulting from the solution of (15) is shown in Fig. 2b. It is seen that in this figure the same singular points appear, but the difference is that the points O and O' transform to stable focuses and damped oscillations occur in the system. The figures indicate the phase trajectories. The iso-

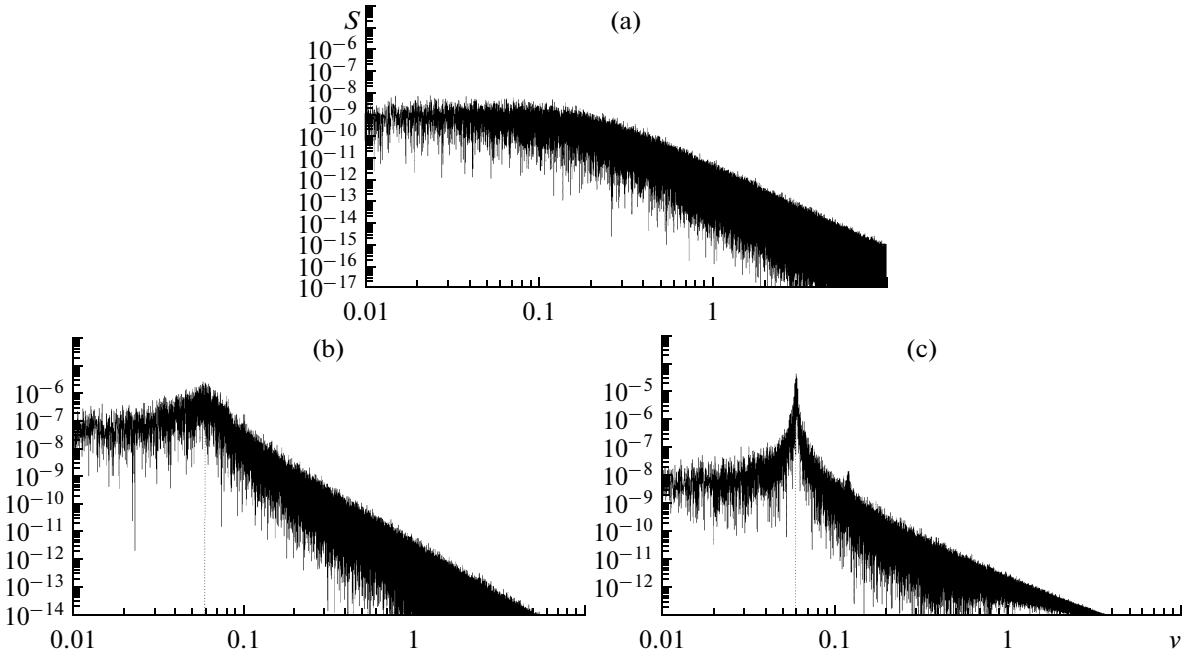

Fig. 5. Spectral power densities that correspond to data shown in Fig. 4.

cline shown by the dotted line differs from the isocline in the previous case.

The corresponding time dependences (Fig. 3b) demonstrate the positive portions along which $\sigma \approx 0$, corresponding to the slow motion of the rubbing surfaces. This is caused by the fact that during the system's evolution the configurative point on the phase-plane portrait passes in the vicinity of the origin ($\sigma \approx 0$) at a low rate of stress variation ($\dot{\sigma} \approx 0$). However, a stationary nonzero value of the stresses σ_0 is always reached, which corresponds to sliding. In this case, no transition to reciprocal motion occurs, which indicates a higher maximum of the potential in the origin.

As in the previous case, the derived dependence $\sigma(t)$ under the effect of noise, which is shown in Fig. 4b, represents the stationary mode, the parameters of which do not change with time. It is seen that the dependence is periodical. To corroborate this fact, we have carried out additional Fourier analysis. It is seen in Fig. 5b that with increasing frequency of the component of the signal, its power decreases, but a peak appears at $\nu \approx 0.06$, proving the presence of the periodical component in $\sigma(t)$. Thus, periodical variations in the stresses operate in the case shown in Fig. 4b; this corresponds to the oscillation process in the system. Transitions between the fluidlike and solidlike lubricant structures occur, resulting in the stick-slip mode. It was assumed earlier that the zero stresses corresponded to the solidlike structure and when the temperature T_e exceeded its critical value the stresses became nonzero and the lubricant melted. In this case the following situation arises. Let the stresses initially be minimal, which corresponds, as earlier, to the solidlike lubricant. If the surfaces start moving, the stresses σ grow (see any ascending portion of the dependence in Fig. 4b). When the stresses exceed the critical value, the lubricant melts. Then the elastic component σ_{el} of the stresses relaxes and the total stresses also decrease (see the descending portion of the dependence). When, owing to relaxation, the value of the stresses becomes insufficient for keeping the lubricant in the fluidlike state, it solidifies and the process repeats. Thus, as earlier, melting occurs at high stresses. We note that the described mode differs from that shown in Fig. 4a. In this case, periodical transitions between the solidlike and fluidlike lubricant structures occur, while Fig. 4a corresponds to the fluidlike structure and the random variations in the stresses seen in it represent fluctuations that do not cause melting or solidification. Since the dependence shown in Fig. 4b is not strictly periodical, this mode corresponds to experiments with chain molecules [1] that hardly form ordered structures; this is why fluctuations are superimposed on oscillations. The amplitude of stick-slip transitions varies. Moreover, the effect of fluctuations may cause the instability of the focus, resulting in continuous increase in the amplitude of stress oscillations, which is similar to resonance in the system.

The case $\tau_\sigma \ll \tau_\varepsilon, \tau_T$. In this case we assume $\tau_\sigma \dot{\sigma} \approx 0$ and measure time in units of τ_ε, yielding

$$\ddot{\sigma} + \left[\left(2A^2\sigma + A\beta - \frac{2A\beta\sigma^\beta}{\alpha^\beta + \sigma^\beta} - \frac{1}{\sigma}\right)\dot{\sigma} + A\sigma\left(1 + \frac{1}{\tau}\right) + \frac{1}{\tau}\right] \times \frac{\dot{\sigma}}{A\sigma + 1} + \frac{B}{A\sigma + 1}\sigma = \xi(t), \quad (16)$$

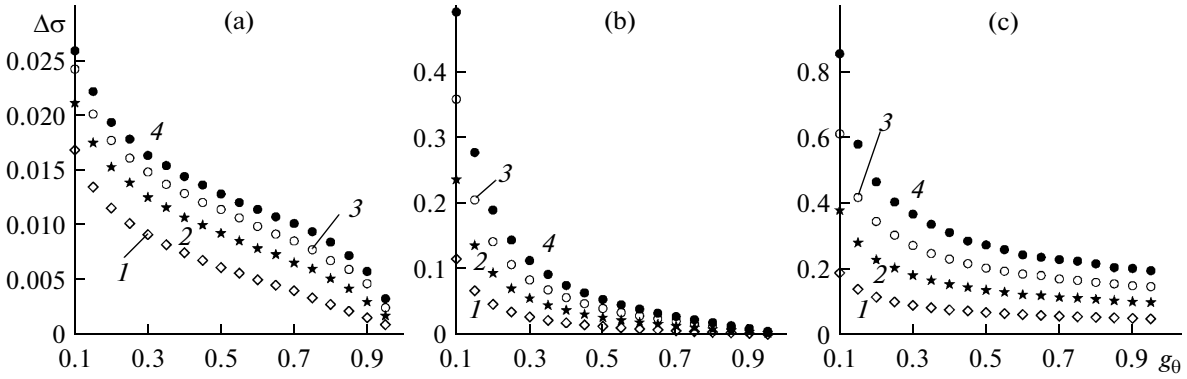

Fig. 6. Dependences of average amplitude of stick-slip transitions on parameter g_θ, which correspond to data shown in Fig. 4, at different values of parameter τ: (*1*) τ = 40; (*2*) 80; (*3*) 120; (*4*) τ = 160.

where $\tau = \tau_T/\tau_\varepsilon$. At this ratio between the relaxation times, before the stationary state is reached, a greater number of oscillations occur around the focus on the phase-plane portrait (Fig. 2c) compared to the previous case. This is also confirmed by Fig. 3c, which illustrates long oscillations that do not attenuate even at $t = 900$. Figure 4c shows the time dependence of the stresses under the effect of noise (in all of the cases under consideration D = const); it is flatter and more regular than that presented in Fig. 4b.

The corresponding spectrum (Fig. 5c) has a much narrower and higher peak at $\nu \approx 0.06$ than the spectrum shown in Fig. 5b; this is why the fundamental frequency is $\nu \approx 0.06$. Figure 4c illustrates the dependence within the time interval $\delta t = 400$, which corresponds, at the above frequency, to 24 full oscillations, which appear on the dependence. It can be concluded that in this case a more time-stable stick-slip mode occurs with a higher amplitude. Thus, one may expect the onset of stick-slip friction in the systems with $\tau_\sigma \ll \tau_\varepsilon \ll \tau_T$. We note that, according to formula (8), at the parameters indicated in Fig. 3 ($\theta = 0.7$, $g_\theta = 0.4$, $\alpha = 0.1$, $\beta = 4$, and $T_e = 25$) in all of the cases under consideration the stationary stress value $\sigma_0 \approx 3.78594$ steadies with time. It is seen in Fig. 4 that the effect of noise may cause slight fluctuations around the stationary value of σ_0 (Fig. 4a) and influence the system critically, thus changing the friction mode (Figs. 4b, c).

NUMERICAL EXPERIMENT

In the previous section, we have shown that the ratio between the relaxation times in the system under consideration affects critically its behavior. Thus, the noise effect may result in fluctuations or periodic stick-slip friction. However, these conclusions are qualitative. To make a quantitative estimate, we carry out the following computer experiment. As earlier, we solve equations (9), (15), and (16), but here we are aiming at determining the average amplitude of stick-slip transitions. To do this, we select the time increment $\Delta t = 0.001$ and solve the equation within the interval $t \in [0, 2000]$ under arbitrary initial conditions without performing experiments. The stationary mode is reached within this interval. Then we assume the time equal to zero and calculate the average stress within the interval $t \in [0, 5000]$. After the next equaling of the time to zero, we calculate the average amplitude within the time interval $t \in [0, 10^6]$ in the following manner. If the stresses exceed their average value, we determine the maximal stress. As soon as the stresses become below their average value, their maximal value is stored and the minimal stress is found. After the next pass over the average stress, the minimal stress is stored and the next maximum is determined, and so on. Then, the sum of all minima is subtracted from the sum of all maxima and the result is divided by the number of maxima. The measurements are carried out within the range of g_θ from 0.1 to 0.95 with an increment of 0.05 for four values of τ; recall that in all of the cases under consideration τ is the ratio of various relaxation times. This method of determining the average amplitude is apparently more adequate for the second and third cases; in the first case it yields an error since the dependence $\sigma(t)$ is not periodical in this case and may undergo frequent rises or drops of the stresses both above the average stress and below it. Nevertheless, the method will be capable of finding the level of fluctuations in this case.

The calculation results are shown in Fig. 6, where the ordinate axis represents the average "excursion" of the stress variation $\Delta\sigma = \langle\sigma_{max}\rangle - \langle\sigma_{min}\rangle$, according to Fig. 4. It is seen that in all cases increase in the parameter τ causes growth of the amplitude of stress oscillations; with increasing parameter g_θ, the amplitude decreases. The figure also corroborates the fact that the most pronounced oscillations occur in the third case and in the second case the amplitude of oscillations decreases. The ratio of the relaxation times that corresponds to the first case causes slight variations in the stresses around their average value. To all appearances, the dependences are smooth, which proves the

sufficient accuracy of measurement and the fact that the selected integration time is sufficient for determining the desired value.

CONCLUSIONS

The results show that the periodical stick-slip friction mode observed experimentally can be described within the limits of the rheological model, which is parametrized by the shear stresses and strain, as well as by the lubricant temperature. The main feature of the mode is that transitions between the fluidlike and solidlike lubricant structures occur at different values of the stresses; this results from the effect of fluctuations on the system, which induces the stick-slip mode. It is shown that the most stable periodical stick-slip mode occurs when the stress relaxation time is the shortest, the temperature relaxation time is the longest, and the strain relaxation time occupies the intermediate position. When the temperature relaxation time is the shortest, the periodical mode cannot occur in the system. This may be caused by quick heat transfer to the friction surfaces during dissipation through heat conductivity. It is found that in all cases, increase in the lubricant shear modulus reduces the amplitude of stick-slip transitions.

ACKNOWLEDGMENTS

This work was supported by the Fundamental Researches State Fund of Ukraine, project nos. F25/668-2007 and F25/97-2008.

DESIGNATIONS

σ—the shear stresses in the lubricating layer; ε—the shear strain in the lubricating layer; T—the lubricant temperature; T_{c0}—the lubricant melting temperature; σ_s—the unit of the stresses σ; ρ—the lubricant density; c_v—the lubricant specific heat; η—the lubricant shear viscosity; η_0—the characteristic value of the lubricant shear viscosity; T_c—critical temperature; τ_T—temperature relaxation time; ε_s—the unit of the shear strain ε; G_0—the characteristic value of the shear modulus; l—the lubricating layer thickness; κ—the thermal conductivity; τ_ε—the relaxation time of the strain ε; τ_σ—the relaxation time of the stresses σ; T_e—the temperature of the friction surfaces; G—the lubricant shear modulus or the slope angle of the loading curve within the Hooke portion; Θ—the strengthening factor or the slope angle of the loading curve within the plastic portion; β—the phenomenological coefficient; σ_p—the phenomenological coefficient; σ_m and ε_m—the maximal values of the shear stresses and the strain within the Hooke portion; $\theta = \Theta/g$—the ratio of the strengthening factor to the shear modulus; $g_\theta = \Theta/G_0$—the ratio of the strengthening factor to the characteristic value of the shear modulus; $\alpha = \sigma_p/\sigma_s$—the phenomenological coefficient; σ_0—the stationary value of the stresses; ε_0—the stationary value of the strains; $\xi(t)$—the delta-correlated stochastic source or white noise; D—the noise intensity; γ—the friction coefficient in the canonical equation of damped oscillations; ω_0—the fundamental frequency of oscillations; $y = \dot{\sigma}$—the time derivative of the stresses; W_n—the random force modeled by the Box–Muller function; r_1 and r_2—uniformly distributed pseudorandom numbers; $S(\nu)$—the spectral density of the power; ν—the frequency; σ_{el}—the elastic component of the shear stresses.

REFERENCES

1. Yoshizawa, H. and Israelachvili, J., Fundamental Mechanisms of Interfacial Friction. 2. Stick-Slip Friction of Spherical and Chain Molecules, *J. Phys. Chem.,* 1993, vol. 97, pp. 11300–11313.
2. Reiter, G., Demirel, A.L., Peanasky, J., Cai, L.L., and Granick, S., Stick to Slip Transition and Adhesion of Lubricated Surfaces in Moving Contact, *J. Chem. Phys.*, 1994, vol. 101, pp. 2606–2615.
3. Demirel, A.L. and Granick, S., Transition from Static to Kinetic Friction in a Model Lubricating System, *J. Chem Phys.*, 1998, vol. 109, pp. 6889–6897.
4. Popov, V.L., Thermodynamics and Kinetics of Melting by Shear of Thin Lubricating Layer between Two Solids, *Zh. Tekh. Fiz.*, 2001, vol. 71, pp. 100–110.
5. Filippov, A.E., Klafter, J., and Urbakh, M., Friction through Dynamical Formation and Rupture of Molecular Bonds, *Phys. Rev. Lett.*, 2004, vol. 92, p. 135503 (4).
6. Tshiprut, Z., Filippov, A.E., and Urbakh, M., Tuning Diffusion and Friction in Microscopic Contacts by Mechanical Excitations, *Phys. Rev. Lett.*, 2005, vol. 95, p. 016101 (4).
7. Khomenko, A.V. and Yushchenko, O.V., Solid-Liquid Transition of Ultrathin Lubricant Film, *Phys. Rev. E.,* 2003, vol. 68, p. 036110 (6).
8. Braun, O.M. and Naumovets, A.G., Nanotribology: Microscopic Mechanisms of Friction, *Surf. Sci. Rep.,* 2006, vol. 60, pp. 79–158.
9. Israelachvili, J., Adhesion Forces between Surfaces in Liquids and Condensable Vapours, *Surf. Sci. Rep.*, 1992, vol. 14, pp. 109–159.
10. Khomenko, A.V. and Lyashenko, I.A., Stochastic Theory of Stick-Slip Mode of Melting of Ultrathin Lubricating Film, *Zh. Tekh. Fiz.*, 2005, vol. 75, pp. 17–25.
11. Khomenko, A.V. and Lyashenko, I.A., Melting of Ultrathin Lubricating Film due to Dissipative Heating of Friction Surfaces, *Zh. Tekh. Fiz.*, 2007, vol. 77, pp. 137–140.
12. Khomenko, A.V. and Lyashenko, I.A., Phase Dynamics and Kinetics of Thin Lubricant Film Driven by Correlated Temperature Fluctuations, *Fluct. Noise Lett.*, 2007, vol. 7, pp. L111–L133.
13. Khomenko, A.V. and Lyashenko, I.A., Temperature Dependence Effect of Viscosity on Ultrathin Lubricant Film Melting, *Phys. Condens. Matter.*, 2006, vol. 9, pp. 695–702.

14. Khomenko, A.V. and Lyashenko, I.A., Hysteresis Phenomena at Melting of Ultrathin Lubricating Film, *Fiz. Tverd. Tela*, 2007, vol. 49, pp. 886–890.

15. Khomenko, A.V. and Lyashenko, I.A., Hysteresis Phenomena at Ultrathin Lubricant Film Melting in the Case of First-Order Phase Transition, *Phys. Lett. A*, 2007, vol. 366, pp. 165–173.

16. *Nanotribology and Nanomechanics*, Bhushan, B., Ed., Berlin: Springer, 2005.

17. Khomenko, A.V. and Prodanov, N.V., Synergetic Kinetics of Melting of Ultrathin Lubricating Film, *Fiz. Tekh. Vysok. Davlenii*, 2006, vol. 16, pp. 164–179.

18. Olemskoi, A.I. and Khomenko, A.V., Tree-Parameter Kinetics of Phase Transition, *Zh. Eksp. Teor. Fiz.*, 1996, vol. 110, pp. 2144–2167.

19. Press, W.H., Flannery, B.P., Teukolsky, S.A., and Vetterling, W.T., *Numerical Recipes in C: the Art of Scientific Computing*, New York: Cambridge University Press, 1992.